

# Estimation of the Influence of GaAs, GaSb and InP Substrates on the Boundaries of Stable Compositions of GaAsSb Ternary Solid Solutions in Epitaxial Layers of Various Thicknesses

A. Gorbatchev\*, F. De Anda, & V. Michournyi

Institute for Research in Optical Communication – UASLP, San Luis Potosí, S.L.P., Mexico

\*Corresponding author: A. Gorbatchev, Institute for Research in Optical Communication – UASLP, San Luis Potosí, S.L.P., Mexico.

Submitted: 26 November 2025 Accepted: 10 December 2025 Published: 31 January 2026

**Citation:** Gorbatchev, A., De Anda, F., & Michournyi, V. (2026). Estimation of the Influence of GaAs, GaSb and InP Substrates on the Boundaries of Stable Compositions of GaAsSb Ternary Solid Solutions in Epitaxial Layers of Various Thicknesses. Nov Joun of Appl Sci Res, 3(1), 01-08.

## Abstract

Various III-V solid solution systems are characterized by the existence of a spinodal decomposition area, which imposes limitations on the formation of epitaxial layers, in particular on their composition and thicknesses. In this work, we have performed a comparative analysis of the change in the stability region boundaries of GaAsSb solid ternary solutions formed on GaAs, GaSb and InP substrates in the temperature range from 400 to 650 °C. The calculations have been completed using the CALPHAD method and the SGTE data. Disregarding the elastic energy generated by the lattice mismatch between forming solid solutions and substrate, the estimations show a continuous spinodal decomposition area, between near pure GaAs and GaSb compositions, that expands with decreasing temperatures. Given the elastic energy contribution to the solid solution energy, extensive regions of stable compositions are always observed in thin epitaxial layers with thicknesses  $d$  on the order of a few monolayers. On GaAs and GaSb substrates these regions shrink rapidly, as the layer grows, to compositions corresponding to free elastic energy solid solutions. On the InP substrate, at large thicknesses, within the spinodal decomposition area, the interval of stable compositions is conserved around the isoperiodic composition with the substrate (GaAs0.51Sb0.49), and for the 500 nm epitaxial layer lies between 0.46-0.66 molar fractions of GaAs. The results obtained may be of interest for the growth of thick layers in heterostructures to obtain photodetectors for the mid-infrared wavelength range.

**Keywords:** Spinodal Decomposition, CALPHAD Modeling, GaAsSb Ternary Solid Solutions, Epitaxial Layers, Elastic Strain Energy.

## Introduction

Ternary GaAsSb solid solutions are characterized by a strong variation in the bandgap, from 0.727 eV for GaSb to 1.42 eV for GaAs, depending on the ratio between As and Sb, covering the electromagnetic wavelength range from 0.873 to 1.7 μm at room temperature [1]. This makes them suitable for the fabrication of solar cells, telecommunication devices, and broadband photodetectors operating from the near to mid infrared range [2, 3]. Nevertheless, the growth of ternary GaAsSb solid solutions is accompanied by a number of challenges. First, this is related to the lattice mismatch with the substrate, as in the case of growth on GaAs substrates, which leads to the formation of crystal defects and, consequently, degradation of their optoelectronic properties. In addition, limitations on the growth of GaAsSb solid solutions of certain compositions arise due to the existence

of a miscibility gap [4]. Theoretical studies together with experimental results show that the spinodal decomposition areas vary with temperature. However, the elastic energy generated in epitaxial layers in the presence of lattice mismatch with the substrate can act as a stabilizing factor for the composition [5]. Its positive contribution decreases in layers of larger thickness. GaAs, GaSb, InP substrates are typically used to grow GaAsSb epitaxial layers [6-11]. In this work, we have analyzed the substrate stabilizing effect of elastic energy and its dependence of the epitaxial layer thickness at temperatures ranging from 400 to 650 °C. We propose to use the CALPHAD method, which has gained wide application in recent years [12]. The accumulated empirical data and achieved thermodynamic assessments make it possible to estimate the free energies of various III-V solid solutions and to analyze their compositional stability.

## Calculation Method

As the thermodynamic stability criterion for the ternary GaAs-ySb1-y compounds, we use the condition based on the second partial derivative of the Gibbs energy with respect to the molar fraction y of GaAs in the solid phase [13].

$$\frac{\partial^2 G}{\partial y^2} \geq 0 \quad (1)$$

The total Gibbs energy  $G^{\text{total}}$  of an epitaxial layer consists of two components: the free-strain solid energy  $G^{\text{S}}$  of the solid phase, and the elastic energy  $G^{\text{el}}$  generated due to the lattice-parameter mismatch with the substrate.

$$G^{\text{total}} = G^{\text{S}} + G^{\text{el}} \quad (2)$$

According to the model of regular solutions, the expression to calculate the strain-free energy of the solid phase [14, 15].

$$G^{\text{S}} = yG_{\text{GaAs}}^{\text{SO}} + (1-y)G_{\text{GaSb}}^{\text{SO}} + RT(y \ln y + (1-y) \ln(1-y)) + y(1-y)L_{\text{GaAs-GaSb}}^{\text{S}} \quad (3)$$

Where  $L_{\text{GaAs-GaSb}}^{\text{S}}$  denotes the interaction parameter of the

**Table 1:** The thermodynamic parameters used in the calculations.

Parameters	Values (J/mol)	Ref.
$H_{\text{Ga}}^{\text{O}}$	5572	(Dinsdale, 1991)
$H_{\text{AS}}^{\text{O}}$	5117.032	(Dinsdale, 1991)
$H_{\text{Sb}}^{\text{O}}$	5870.152	(Dinsdale, 1991)
$\text{GHSER}_{\text{GaAs}}$	$-104352 + 265.43256T - 48.681258T\ln T - 1.1158 \times 10^{-3} T^2 + 127670 \times T^{-1} - 7.1378 \times 10^{-7} T^3$	(Li, 1998)
$\text{GHSER}_{\text{GaSb}}$	$-59774.701 + 267.809609T - 51.1966138T\ln T + 5.14355 \times 10^{-3} T^2 - 17707 \times T^{-1} - 3.043588 \times 10^{-6} T^3 + 1.645 \times 10^{23} T^9$	(Li, 1998)
$L_{\text{GaAs-GaSb}}^{\text{S}}$	$24824 - 7.74301T + 4774(2y-1)$	(Li, 1998)

$$G^{\text{el}} = \frac{\mu(1+\nu)}{2(1-\nu)} N_A a^3 f^2 \quad (h < h_{\text{cr}}) \quad (5)$$

$$G^{\text{el}} = \frac{N_A a^3}{4h} \Delta \left( 1 + \ln \frac{h}{h_{\text{cr}}} \right) \quad (h \geq h_{\text{cr}}) \quad (6)$$

The critical thickness  $h_{\text{cr}}$  is calculated from

$$h_{\text{cr}} = \frac{\Delta}{2\mu f^2} \frac{1-\nu}{1+\nu} \quad (7)$$

A value of  $\Delta=0.8 \text{ J/m}^2$  was used for the energy barrier, corresponding to growth on (001)-oriented substrates.

The lattice misfit parameter f is given by

$$f = \frac{a - a_s}{a_s} \quad (8)$$

The lattice constant of epitaxial layer, a, is described by the Vegard's law

$$a = ya_{\text{GaAs}} + (1-y)a_{\text{GaSb}} \quad (9)$$

where  $a_{\text{GaAs}}$  and  $a_{\text{GaSb}}$  are lattice parameters of binary GaAs and GaSb solid compounds.  $a_s$  is the lattice parameter of the substrate. The Poisson ratio  $\nu$  and the shear modulus  $\mu$  of the ternary solid solutions were calculated using the following equations [18].

**Table 2:** Elastic parameters for binary compounds [1].

Binary compound	Lattice constant (Å)	$C_{11}$ (GPa)	$C_{12}$ (GPa)	$C_{44}$ (GPa)
GaAs	5.65325	1221	566	600
GaSb	6.0959	884.2	402.6	432.2

pseudobinary system in the solid phase.  $G_{\text{GaAs}}^{\text{SO}}$  and  $G_{\text{GaSb}}^{\text{SO}}$  are the Gibbs energies of the GaAs and GaSb binary solid phases, respectively, calculated using expressions that include the enthalpies  $H_i^0$  of the stable state of the constituent pure elements at 298.15 K, as well as empirical temperature-dependent functions  $\text{GHSER}_{ij}$  [16].

$$G_{ij}^{\text{SO}} = H_i^0 + H_j^0 + \text{GHSER}_{ij} \quad (4)$$

The elastic energy  $G^{\text{el}}$ , assuming the formation of planar films, was calculated using the Ohtani's procedure, that allows one to obtain its dependence on the epitaxial layer thickness h depending on whether this thickness exceeds the critical value  $h_{\text{cr}}$  or not [17].

The thermodynamic parameters used in the present calculations are listed in Table 1.

$$\nu = y\nu_{\text{GaAs}} + (1-y)\nu_{\text{GaSb}} \quad (10)$$

$$\mu = \frac{y\mu_{\text{GaAs}} a_{\text{GaAs}} + (1-y)\mu_{\text{GaSb}} a_{\text{GaSb}}}{a} \quad (11)$$

The corresponding  $\nu_{ij}$  and  $\mu_{ij}$  of the binary solid phases were expressed through their elastic stiffness parameters  $C_{11}$ ,  $C_{12}$ ,  $C_{44}$  and elastic compliance constants  $S_{11}$ ,  $S_{12}$  in the cubic system [17].

$$\mu_{ij} = \frac{C_{44}^{(ij)}}{2} \quad (12)$$

$$\nu_{ij} = \frac{S_{12}^{(ij)}}{S_{11}^{(ij)}} \quad (13)$$

$$S_{11} = \frac{C_{11} + C_{12}}{(C_{11} - C_{12})(C_{11} + 2C_{12})} \quad (14)$$

$$S_{12} = \frac{C_{12}}{(C_{11} - C_{12})(C_{11} + 2C_{12})} \quad (15)$$

The elastic parameters for the binary compounds are summarized in Table 2.

## Results

Using Eq. (3), we first obtained the Gibbs free-energy curves for

strain-free GaAsSb solid solutions as a function of their compositions at temperatures of 450, 550, and 650 °C.

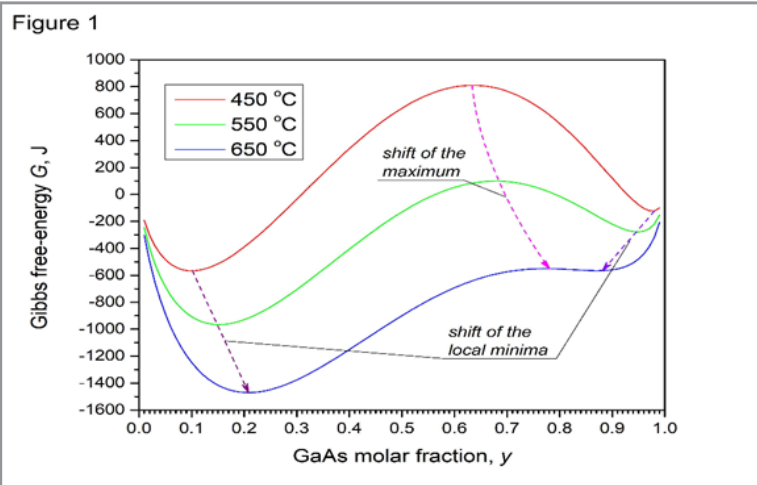


**Figure 1:** Gibbs free-energy  $G$  curves of ternary GaAsSb solid solutions as a function of GaAs molar fraction  $y$  at 450 °C, 550 °C, and 650 °C.

These dependencies are characterized by the presence of a maximum that shifts with increasing temperature approximately from the value of GaAs molar fraction  $y=0.64$  at 450 °C to  $y=0.77$  at 650 °C. Two local minima are located near the binary GaAs and GaSb compounds. As the temperature increases, the minima move closer to the central maximum. Such behavior of the Gibbs

free energy as a function of composition indicates the existence of an area of instable ternary solid solutions of the system under consideration, shown in Fig. 2 as a white field. The immiscibility area is asymmetric and shifted toward the GaAs-rich side, and it narrows at higher temperatures, which qualitatively agrees with the results reported by [4].

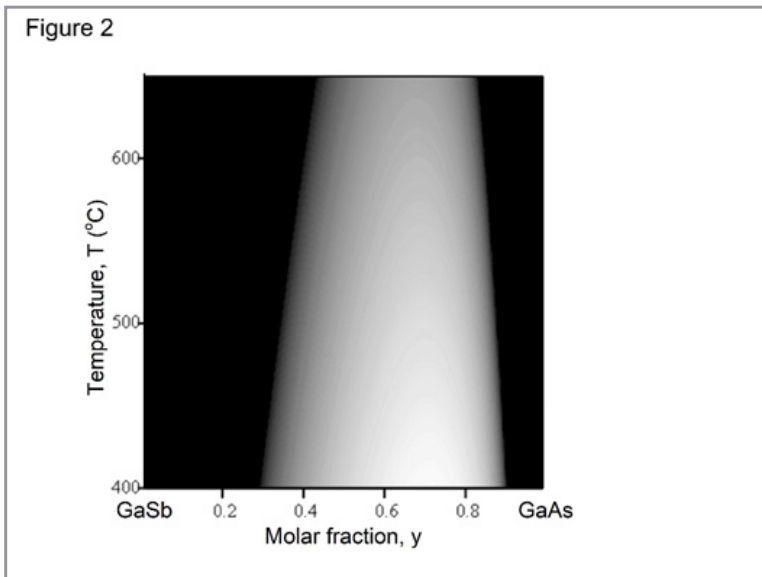


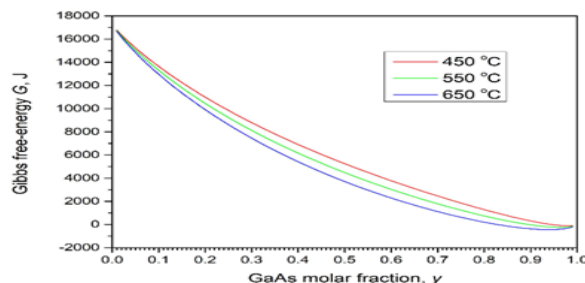
**Figure 2:** Decomposition area (light area) of strain-free GaAsSb solid solutions in the temperature range from 400 °C to 650 °C.

In practice, the formation of solid solutions is carried out on crystalline substrates. Lattice-parameter mismatch at the initial stages of growth may lead to the formation of planar strained

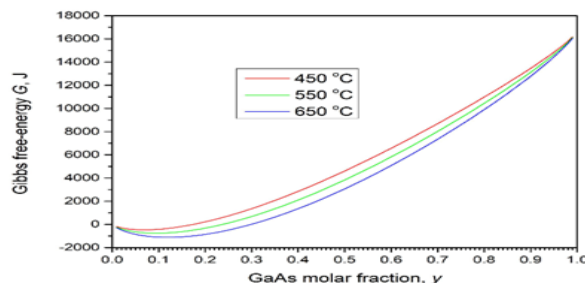
epitaxial layers, with the associated elastic energy contributing to the total energy and reaching its maximum value when the layer thickness is below the critical thickness.

**Figure 3**

a) On a GaAs substrate



b) On a GaSb substrate



c) On a InP substrate

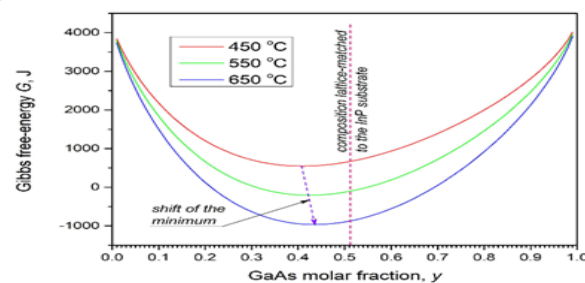


**Figure 3:** Total Gibbs free-energy curves of ternary GaAsSb solid solutions as a function of GaAs molar fraction  $y$  at 450 °C, 550 °C, and 650 °C for epitaxial layers with the thicknesses  $h$  below the critical thickness  $h_{cr}$ , formed on (a) on GaAs, (b) GaSb and c) InP substrates.

In the case of epitaxial growth on GaAs and GaSb substrates, incorporation of the elastic-energy contribution, corresponding to its maximum value in the regime of coherent planar films (Figs. 3a and 3b), leads to Gibbs free-energy profiles that exhibit an almost monotonic increase toward the composition range mismatched with the substrate. Under these conditions, only shallow minima are preserved, located in close proximity to the compositions that are lattice-matched to the respective substrates. This behavior reflects the strong destabilizing influence of the lattice misfit, which suppresses the formation of compositionally distinct stable states across most of the ternary system.

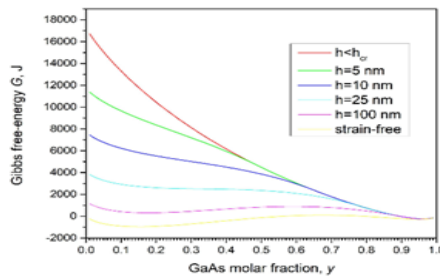
For epitaxial layers grown on InP, a more pronounced minimum in the Gibbs-energy curve appears at a GaAs molar fraction of approximately  $y=0.4$  at 450 °C (red line in Fig. 3c). With increasing temperature, this minimum shifts toward higher values of  $y$ , i.e., toward compositions with a higher As content. At 650 °C (blue curve in Fig. 3c), the minimum moves to approximately  $y=0.44$ , approaching the composition  $\text{GaAs}_0.513\text{Sb}_0.487$  that is lattice-matched to the InP substrate.

Across the entire temperature interval examined, no inflection points are observed in the Gibbs-energy functions. The absence of such curvature changes indicates that the incorporation of elastic energy eliminates the spinodal region throughout the full composition range between the binary endpoints GaAs and GaSb. Consequently, the elastic term acts as a robust stabilizing factor for the GaAsSb solid solution, grown on InP substrates. The thermodynamically preferred composition is consistently pulled toward the lattice-matched value imposed by the substrate.

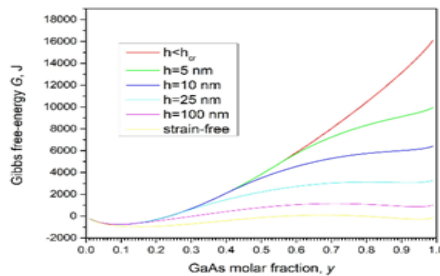
It is important to note that the Gibbs-energy dependencies discussed above correspond to epitaxial layers with thicknesses  $h$  below the critical value  $h_{cr}$ , for which strain relaxation proceeds without the formation of misfit dislocations. When  $h>h_{cr}$  the elastic-energy contribution decreases because of the formation of misfit dislocations. This reduction is expected to occur first for the compositions that exhibit the largest mismatch with the substrate, even at small thicknesses on the order of a few nanometers.

**Figure 4**

a) On a GaAs substrate



b) On a GaSb substrate



c) On a InP substrate

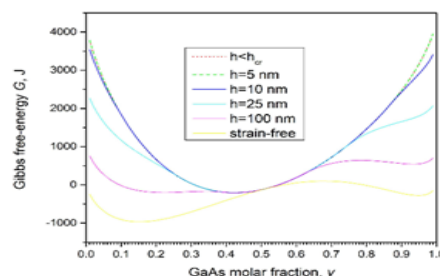


**Figure 4:** Total Gibbs free energy curves of ternary GaAsSb solid solutions as a function of GaAs molar fraction  $y$  at 450 °C, 550 °C, and 650 °C for epitaxial layers formed on (a) on GaAs, (b) GaSb and c) InP substrates.

For GaAs substrates, a significant reduction of the total Gibbs energy in the solid phase is observed at a layer thickness of 5 nm for compositions within the range  $0 \leq y \leq 0.42$  (Fig. 4a). On GaSb substrates, a similar reduction occurs for  $0.6 \leq y \leq 0$  (Fig. 4b), since the corresponding critical thickness values for these compositions are below 5 nm (Fig. 5). For epitaxial layers grown on InP, a splitting in the Gibbs-energy curves appears only at larger thicknesses, around 10 nm (Fig. 4c) corresponding to

compositions more distant from the lattice-matched value on either side. Within the GaAsSb-InP system, the minimum values of the critical thickness are higher compared to those for layers formed on GaAs or GaSb (Fig. 5). This behavior arises from the smaller maximum lattice mismatch with the substrate, which reduces the driving force for strain relaxation and shifts the onset of elastic-energy reduction to larger thicknesses.

**Figure 5**

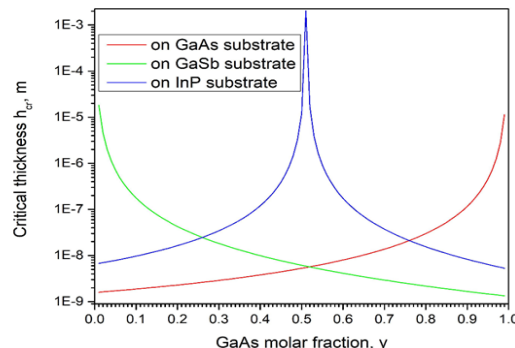


**Figure 5:** Critical thickness  $h_{cr}$  as a function of the GaAs molar fraction for GaAsSb epitaxial layers grown on GaAs (red line), GaSb (green line) and InP (violet line) substrates.

These results should demonstrate that the interplay between lattice mismatch, critical thickness, and elastic-energy relaxation must be explicitly considered in thermodynamic assessments of composition stability in ternary GaAsSb epitaxial layers.

For epitaxial layers grown on GaAs substrates, all ternary compositions remain thermodynamically stable at thicknesses below 5 nm. However, when the thickness exceeds 5 nm, a region of unstable solid solutions appears (light area in Fig. 6), located near the edge of the diagram opposite to the substrate composi-

tion at a molar fraction of  $y \approx 0.20$  at  $400^\circ\text{C}$  and  $y \approx 0.25$  at  $650^\circ\text{C}$ . It should be noted that these compositions are stable in the absence of elastic energy. Increasing the epitaxial layer thickness leads to a gradual widening of the instability region and its shift toward the substrate composition. On GaAs, this shift reaches  $y \approx 0.95$  for thicknesses of about 300 nm at  $400^\circ\text{C}$  and  $y \approx 0.92$  for thicknesses around 150 nm at  $650^\circ\text{C}$ . Further increases in thickness result in a narrowing of the instability region back to the limits characteristic of the strain-free state (yellow hatch area in Fig. 6).

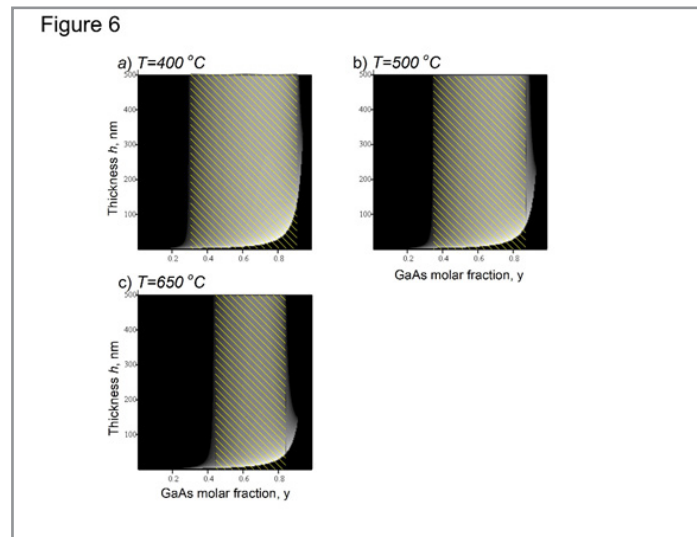


**Figure 6:** Regions of unstable GaAsSb solid phases (light areas) for epitaxial layers with the thicknesses up to 500 nm formed on GaAs substrate at temperatures of (a) 400 °C, (b) 500 and (c) 650 °C. The yellow hatched areas represent the spinodal decomposition domains of the strain-free solid phases.

Importantly, the position of the boundary on the substrate side remains nearly unchanged with temperature up to the point of maximal widening. A similar qualitative behavior is observed for epitaxial layers grown on GaSb substrates, as shown in Fig. 7. For thicknesses below 5 nm, all ternary compositions remain stable. Instability first appears at compositions  $y \approx 0.93$  at  $400^\circ\text{C}$  and  $y \approx 0.87$  at  $650^\circ\text{C}$ . As the layer becomes thicker, the

instability region widens and shifts toward the substrate composition. The left boundary of this region reaches  $y \approx 0.13$  at  $400^\circ\text{C}$  for a layer thickness of about 100 nm and  $y \approx 0.20$  at  $650^\circ\text{C}$  for thicknesses around 45 nm. However, unlike the case of GaAs, a rapid contraction of the spinodal decomposition region occurs at larger thicknesses, and by approximately 300 nm its size approaches that expected in the strain-free state.

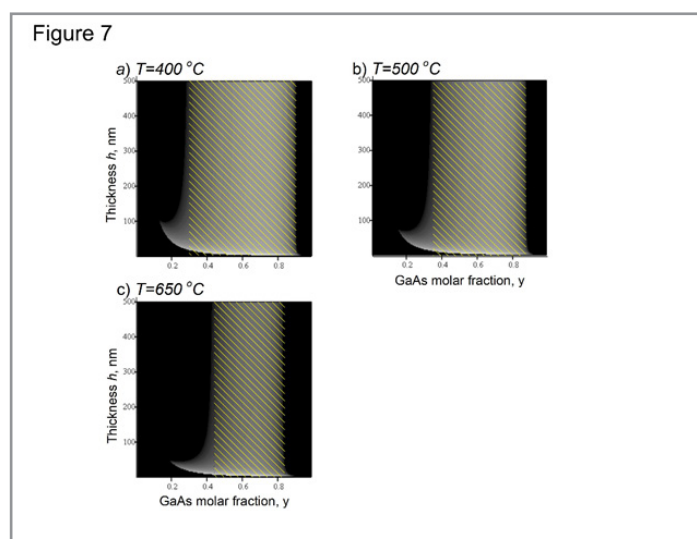


**Figure 7:** Regions of unstable GaAsSb solid phases (light areas) for epitaxial layers with the thicknesses up to 500 nm formed on GaSb substrate at temperatures of (a) 400 °C, (b) 500 and (c) 650 °C. The yellow hatched areas represent the spinodal decomposition domains of the strain-free solid phases.

The most distinctive behavior of the instability regions is observed for layers grown on InP substrates. Instability first develops at thicknesses of about 7 nm for the composition  $y \approx 0.95$  on the GaAs side and at about 14 nm for  $y \approx 0.16$  on the GaSb side (Fig. 8a). With increasing thickness and temperature, the extreme boundaries of the instability region gradually contract. However, on the GaSb side they never reach the limits corresponding to the absence of elastic energy. A key feature is the formation of a symmetric channel of stable compositions around

the value lattice-matched to the substrate. As the epitaxial layer becomes thicker, this channel narrows but does not disappear entirely. According to our estimates, at a thickness of approximately 500 nm, its width is about  $\pm 0.05$  in molar fraction of GaAs around the composition matched to InP (Fig. 8). It is important to emphasize that the dependence of the channel width on layer thickness is the same for all temperatures considered. Only the peripheral boundaries of the instability region shift inward at higher temperatures.

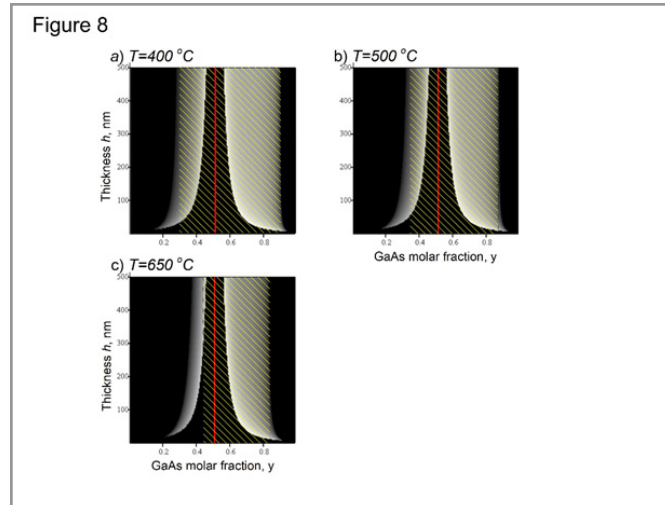


**Figure 8:** Regions of unstable GaAsSb solid phases (light areas) for epitaxial layers with the thicknesses up to 500 nm formed on InP substrate at temperatures of (a) 400 C, (b) 500 and (c) 650 C. The yellow hatched areas represent the spinodal decomposition domains of the strain-free solid phases. The red vertical line corresponds to the ternary solid composition that is lattice-matched to the InP substrate.

## Discussions

The results obtained may have very important practical implications for the growth of epitaxial layers by MBE/MOCVD. On GaAs and GaSb substrates, instability first emerges far from the substrate composition and expands as the layer thickness increases, before eventually returning to the bulk (strain-free) stability limits. Growth must therefore be tightly controlled within a narrow range of stable compositions at intermediate thicknesses in order to avoid strain-induced phase separation.

The strain term is minimized only at the composition that is perfectly lattice-matched to the substrate, which for InP corresponds to approximately 0.51. The strain energy increases as the composition deviates from this point. In combination with this effect, the  $G^{\text{el}}$  contribution produces a sharp, deep minimum at the isoperiodic composition, effectively lowering the  $G^{\text{tot}}$  curve and creating a stable “well” precisely where the bulk system is most unstable.

The most important result is that this stability channel, although it narrows with increasing layer thickness, never disappears completely. This means that even in relatively thick layers (up to the calculated 500 nm), there always exists a composition range around the ideal lattice match that remains thermodynamically resistant to spinodal decomposition.

The persistence of this channel is maintained because the strain term continues to dominate in the vicinity of the lattice-matched composition, even when the overall strain energy in the layer is partially relaxed through the formation of misfit dislocations.

On an InP substrate, the stable channel is preserved around the desired isoperiodic composition. This is the optimal scenario: the thermodynamic driving force strongly promotes the formation of high-quality, compositionally homogeneous material near the lattice-matched target, enabling a broader range of accessible compositions and layer thicknesses without triggering spinodal decomposition.

## Conclusions

Using the CALPHAD method and SGTE thermodynamic data, we constructed Gibbs free energy dependences for GaAsSb solid solutions over the full compositional range. When the elastic contribution associated with lattice match is included the characteristics of these dependences change significantly, and resulting stability regions vary strongly on the substrate on which the solid solutions are formed. The incorporation of elastic energy produces pronounced reduction in total Gibbs energy close to the lattice-matched composition, thereby a stabilizing effect on the compositions of epitaxial layers. The boundaries of stable solution regions become substantially narrower for epitaxial layers with thicknesses up to  $\sim 50$  nm, while the changes show almost no temperature dependence. The most notable and technologically relevant behavior arises for GaAsSb layers grown on InP substrates. The strain-modified free-energy surface exhibits a well-defined stability channel centered on the lattice-matched composition, ensuring local thermodynamic stability. Importantly, this stability channel persists even at large thicknesses on the order of several hundred nanometers. This implies that a finite composition range surrounding the InP-matched value remains resistant to spinodal decomposition, even in thick epitaxial layers. These results indicate that both lattice-matched and

metamorphic GaAsSb layers with high Sb content can be grown on InP while maintaining thermodynamic stability against phase separation. This finding is particularly significant for the design of heterostructures intended for far-infrared and long-wavelength device applications, where high-Sb-content GaAsSb alloys are required.

### Conflict of Interest Statement

The authors declare that there are no academic or financial conflicts of interest that could have influenced the interpretation of the results.

### Acknowledgments

This work was partially supported at UASLP by CONAH-CYT-Mexico and SEP-PRODEP.

### References

1. Vurgaftman, I., Meyer, J. R., & Ram-Mohan, L. R. (2001). Band parameters for III–V compound semiconductors and their alloys. *Applied Physics Reviews*, 89(11), 5815–5875. <https://doi.org/10.1063/1.1368156>
2. Luo, T., Liang, B., Liu, Z., Xie, X., Lou, Z., & Shen, G. (2015). Single GaSb nanowire-based room-temperature photodetectors with broad spectral response. *Science Bulletin*, 60, 101–108. <https://doi.org/10.1007/s11434-014-0687-6>
3. Ishida, K., Shimura, T., Nomura, T., Ohtani, H., & Nishizawa, T. (1988). Phase diagram of the GaAs–Sb system. *Journal of the Less-Common Metals*, 142, 135–144. [https://doi.org/10.1016/0022-5088\(88\)90170-1](https://doi.org/10.1016/0022-5088(88)90170-1)
4. Ipatova, I. P., Malyshkin, V. G., Maslov, A. Yu., & Shchukin, V. A. (1993). Formation of periodic structures with composition modulation during coherent phase separation in quaternary AlIII–BV semiconductor solid solutions. *Fizika i Tekhnika Poluprovodnikov* (Soviet Physics—Semiconductors), 27(2), 285–298.
5. Lu, D. C., Liu, X., Wang, D., & Lin, L. (1992). Growth of GaSb and GaAsSb in the single-phase region by MOVPE. *Journal of Crystal Growth*, 124(1–4), 383–388. [https://doi.org/10.1016/0022-0248\(92\)90488-5](https://doi.org/10.1016/0022-0248(92)90488-5)
6. Yano, M., Ashida, M., Kawaguchi, A., Iwai, Y., & Inoue, M. (1989). Molecular beam epitaxial growth and interface characteristics of GaAsSb on GaAs substrates. *Journal of Vacuum Science & Technology B*, 7(2), 199–203. <https://doi.org/10.1116/1.584716>
7. Donchev, V., Milanova, M., Kirilov, K., Georgiev, S., Kostov, K. L., Piana, G. M., & Avdeev, G. (2021). Low-temperature LPE growth and characterization of GaAsSb layers for photovoltaic applications. *Journal of Crystal Growth*, 574, 126335. <https://doi.org/10.1016/j.jcrysGro.2021.126335>
8. Gao, X., Wei, Z., Zhao, F., Yang, Y., Chen, R., Fang, X., Tang, J., Fang, D., Wang, D., Li, R., Ge, X., Ma, X., & Wang, X. (2016). Investigation of localized states in GaAs–Sb epilayers grown by molecular beam epitaxy. *Scientific Reports*, 6, 29112. <https://doi.org/10.1038/srep29112>
9. Chu, Y., Sang, Y., Liu, Y., Liu, Y., Xu, Z., Chen, J., Liu, F., Li, S., Sun, B., & Wang, X. (2021). Reduced thermal conductivity of epitaxial GaAsSb on InP due to lattice-mismatch-induced biaxial strain. *Journal of Applied Physics*, 130(1), 015106. <https://doi.org/10.1063/5.0049136>
10. Sharma, A. S., Subhasis, D., & Dhar, S. (2020). Control of the composition and the structural properties of GaAs–Sb layers grown by liquid phase epitaxy by Bi addition to the growth melt. *Journal of Crystal Growth*, 545, 125739. <https://doi.org/10.1016/j.jcrysGro.2020.125739>
11. Lukas, H. L., Weiss, J., & Henig, E. T. (1982). Strategies for the calculation of phase diagrams. *CALPHAD: Computer Coupling of Phase Diagrams and Thermochemistry*, 6(3), 229–251. [https://doi.org/10.1016/0364-5916\(82\)90004-9](https://doi.org/10.1016/0364-5916(82)90004-9)
12. Cahn, J. W. (1962). On spinodal decomposition in cubic crystals. *Acta Metallurgica*, 10(3), 179–183. [https://doi.org/10.1016/0001-6160\(62\)90069-4](https://doi.org/10.1016/0001-6160(62)90069-4)
13. Hillert, M., & Staffansson, L. (1970). The regular solution model for stoichiometric phases and ionic melts. *Acta Chemica Scandinavica*, 24, 3618–3626. <https://doi.org/10.3891/acta.chem.scand.24-3618>
14. Dutta, P. S., & Miller, T. R. (2000). Engineering phase formation thermochemistry for crystal growth of homogeneous ternary and quaternary III–V compound semiconductors from melts. *Journal of Electronic Materials*, 29(7), 956–963. <https://doi.org/10.1007/s11664-000-0188-z>
15. Ansara, I., Chatillon, C., Lukas, H. L., Nishizawa, T., Ohtani, H., Ishida, K., Hillert, M., Sundman, B., Argent, B. B., Watson, A., Chart, T. G., & Anderson, T. (1994). A binary database for III–V compound semiconductor systems. *CALPHAD: Computer Coupling of Phase Diagrams and Thermochemistry*, 18(2), 177–222. [https://doi.org/10.1016/0364-5916\(94\)90027-2](https://doi.org/10.1016/0364-5916(94)90027-2)
16. Ohtani, H., Kobayashi, K., & Ishida, K. (2001). Thermodynamic study of phase equilibria in strained III–V alloy semiconductors. *Journal of Phase Equilibria*, 22(3), 276–286.
17. Andreev, V. M., Khvostikov, V. P., Paleeva, E. V., Sorokina, S. V., & Shvarts, M. Z. (1996). GaAs- and GaSb-based solar cells for concentrator and thermophotovoltaic applications. *Proceedings of the 25th IEEE Photovoltaic Specialists Conference*, 143–146.
18. Giri, A. K., & Mitra, G. B. (1986). Theoretical prediction of elastic constants of mixed systems. *physica status solidi (b)*, 134(1), K11–K14. <https://doi.org/10.1002/pssb.2221340142>
19. Dinsdale, A. T. (1991). SGTE data for pure elements. *CALPHAD: Computer Coupling of Phase Diagrams and Thermochemistry*, 15(4), 317–425. [https://doi.org/10.1016/0364-5916\(91\)90030-N](https://doi.org/10.1016/0364-5916(91)90030-N)
20. Li, J.-B., Zhang, W., Li, C., & Du, Z. (1998). A thermodynamic assessment of the Ga–As–Sb system. *Journal of Phase Equilibria*, 19(5), 466–472. <https://doi.org/10.1361/105497198770341950>

**Copyright:** ©2026 A. Gorbatchev, et al. This is an open-access article distributed under the terms of the Creative Commons Attribution License, which permits unrestricted use, distribution, and reproduction in any medium, provided the original author and source are credited.